Simultaneous multi-impairment monitoring of 640 Gb/s signals using photonic chip based RF spectrum analyzer

T. D. Vo[1], M. D. Pelusi[1], J. Schröder[1], F. Luan[1], S. J. Madden[2], D.-Y. Choi[2], D. A. P. Bulla[2], B. Luther-Davies[2], and B. J. Eggleton[1]*

[1] *ARC Centre for Ultrahigh bandwidth Devices for Optical Systems (CUDOS), Institute of Photonics and Optical Science (IPOS), School of Physics, University of Sydney, New South Wales 2006, Australia*
[2] *ARC Centre for Ultrahigh bandwidth Devices for Optical Systems (CUDOS), Laser Physics Centre, Australian National University, Canberra ACT 0200, Australia*
egg@physics.usyd.edu.au

Abstract: We report the first demonstration of simultaneous multi-impairment monitoring at ultrahigh bitrates using a THz bandwidth photonic-chip-based radio-frequency (RF) spectrum analyzer. Our approach employs a 7 cm long, highly nonlinear ($\gamma \approx 9900$ /W/km), dispersion engineered chalcogenide planar waveguide to capture the RF spectrum of an ultrafast 640 Gb/s signal, based on cross-phase modulation, from which we numerically retrieve the autocorrelation waveform. The relationship between the retrieved autocorrelation trace and signal impairments is exploited to simultaneously monitor dispersion, in-band optical signal to noise ratio (OSNR) and timing jitter from a single measurement. This novel approach also offers very high OSNR measurement dynamic range (> 30 dB) and is scalable to terabit data rates.

OCIS codes: (070.4340) Nonlinear optical signal processing; (190.4360) Nonlinear optics, devices; (320.7110) Ultrafast nonlinear optics.

References and links

1. D. C. Kilper, R. Bach, D. J. Blumenthal, D. Einstein, T. Landolsi, L. Ostar, M. Preiss, and A. E. Willner, "Optical Performance Monitoring," J. Lightwave Technol. **22**(1), 294–304 (2004).
2. Z. Pan, C. Yu, and A. E. Willner, "Optical performance monitoring for the next generation optical communication networks," Opt. Fiber Technol. **16**(1), 20–45 (2010).
3. B. Fu, and R. Hui, "Fiber Chromatic Dispersion and Polarization-Mode Dispersion Monitoring Using Coherent Detection," IEEE Photon. Technol. Lett. **17**(7), 1561–1563 (2005).
4. F. N. Hauske, M. Kuschnerov, B. Spinnler, and B. Lankl, "Optical Performance Monitoring in Digital Coherent Receivers," J. Lightwave Technol. **27**(16), 3623–3631 (2009).
5. T. B. Anderson, A. Kowalczyk, K. Clarke, S. D. Dods, D. Hewitt, and J. C. Li, "Multi Impairment Monitoring for Optical Networks," J. Lightwave Technol. **27**(16), 3729–3736 (2009).
6. L. Baker-Meflah, B. Thomsen, J. Mitchell, and P. Bayvel, "Simultaneous chromatic dispersion, polarization-mode-dispersion and OSNR monitoring at 40Gbit/s," Opt. Express **16**(20), 15999–16004 (2008).
7. C. J. Youn, K. J. Park, J. H. Lee, and Y. C. Chung, "OSNR Monitoring Technique Based on Orthogonal Delayed-Homodyne Method," IEEE Photon. Technol. Lett. **14**(10), 1469–1471 (2002).
8. M. N. Petersen, Z. Pan, S. Lee, S. A. Havstad, and A. E. Willner, "Online Chromatic Dispersion Monitoring and Compensation Using a Single Inband Subcarrier Tone," IEEE Photon. Technol. Lett. **14**(4), 570–572 (2002).
9. G. P. Agrawal, *Nonlinear Fiber Optics,* 3rd ed. (California: Academic Press, 2001).
10. C. Dorrer, and D. N. Maywar, "RF Spectrum Analysis of Optical Signals Using Nonlinear Optics," J. Lightwave Technol. **22**(1), 266–274 (2004).
11. M. Pelusi, F. Luan, T. D. Vo, M. R. E. Lamont, S. J. Madden, D. A. Bulla, D. Y. Choi, B. Luther-Davies, and B. J. Eggleton, "Photonic-chip-based radio-frequency spectrum analyser with terahertz bandwidth," Nat. Photonics **3**(3), 139–143 (2009).
12. T. T. Ng, J. L. Blows, J. T. Mok, R. W. McKerracher, and B. J. Eggleton, "Cascaded Four-Wave Mixing in Fiber Optical Parametric Amplifiers: Application to Residual Dispersion Monitoring," J. Lightwave Technol. **23**(2), 818–826 (2005).
13. P. Vorreau, D. C. Kilper, and J. Leuthold, "Optical Noise and Dispersion Monitoring With SOA-Based Optical 2R Regenerator," IEEE Photon. Technol. Lett. **17**(1), 244–246 (2005).

#119870 - $15.00 USD Received 11 Nov 2009; revised 28 Jan 2010; accepted 9 Feb 2010; published 12 Feb 2010

14. R. Adams, M. Rochette, T. T. Ng, and B. J. Eggleton, "All-Optical In-Band OSNR Monitoring at 40 Gb/s Using a Nonlinear Optical Loop Mirror," IEEE Photon. Technol. Lett. **18**(3), 469–471 (2006).
15. M. Dinu, D. C. Kilper, and H. R. Stuart, "Optical Performance Monitoring Using Data Stream Intensity Autocorrelation," J. Lightwave Technol. **24**(3), 1194–1202 (2006).
16. T. D. Vo, M. D. Pelusi, J. Schröder, B. Corcoran, and B. J. Eggleton, "Multi-Impairment Monitoring at 320 Gb/s based on Cross Phase Modulation Radio-Frequency Spectrum Analyzer," IEEE Photon. Technol. Lett. in press.
17. J. P. Curtis, and J. E. Carroll, "Autocorrelation systems for the measurement of picosecond pulses from injection lasers," Int. J. Electron. **60**(1), 87–111 (1986).
18. M. D. Pelusi, T. D. Vo, F. Luan, S. J. Madden, D.-Y. Choi, D. A. P. Bulla, B. Luther-Davies, and B. J. Eggleton, "Terahertz bandwidth RF spectrum analysis of femtosecond pulses using a chalcogenide chip," Opt. Express **17**(11), 9314–9322 (2009).
19. D. V. D. Linde, "Characterization of the Noise in Continuously Operating Mode-Locked Lasers," Appl. Phys. B **39**(4), 201–217 (1986).
20. J. Fatome, J. Garnier, S. Pitois, M. Petit, G. Millot, M. Gay, B. Clouet, L. Bramerie, and J.-C. Simon, "All-optical measurements of background, amplitude, and timing jitters for high speed pulse trains or PRBS sequences using autocorrelation function," Opt. Fiber Technol. **14**(1), 84–91 (2008).
21. J. Dörring, G. B. Tudury, A. Lenihan, G. M. Carter, and Y. J. Chen, "All-optical timing jitter measurements on 40 Gbit/s pseudorandom RZ data after long-haul transmission in dispersion-managed soliton system," Electron. Lett. **38**(14), 727–729 (2002).
22. M. A. F. Roelens, S. Frisken, J. A. Bolger, D. Abakoumov, G. Baxter, S. Poole, and B. J. Eggleton, "Dispersion Trimming in a Reconfigurable Wavelength Selective Switch," J. Lightwave Technol. **26**(1), 73–78 (2008).
23. S. Atkins, and B. Fischer, "All-Optical Pulse Rate Multiplication Using Fractional Talbot Effect and Field-to-Intensity Conversion With Cross-Gain Modulation," IEEE Photon. Technol. Lett. **15**(1), 132–134 (2003).
24. J. Hancock and S. Draving, "Jitter - Understanding It, Measuring It, Eliminating It. Part 2: Jitter Measurements," High Freq. Electron., 20–28 (2004).
25. H. N. Ereifej, R. Holzlohner, G. A. Carter, and C. R. Menyuk, "Intersymbol Interference and Timing Jitter Measurements in a 40-Gb/s Long-Haul Dispersion-Managed Soliton System," IEEE Photon. Technol. Lett. **14**(3), 343–345 (2002).

1. Introduction

Optical performance monitoring (OPM) is essential for next generation reconfigurable optical communication systems. Typical roles for OPM include enabling both quality of service and fault management in highly transparent networks [1,2]. For example OPM is used to monitor transmitted signals and quantify their degradation. These monitoring features are then exploited for impairment mitigation, or to trigger alarms for traffic re-routing. Ultimately an OPM scheme that can provide high sensitivity to impairments and multi-impairment monitoring capability at all operating bitrates is highly desirable.

Current OPM methods based on conventional opto-electronic devices, such as coherent detection [3,4], asynchronous delay tap sampling [5], in-band tone monitoring [6], orthogonal delayed-homodyne [7] and single in-band subcarrier tone methods [8] are mature and relatively effective for the measurement of signal impairments. These techniques, however, rely on fast opto-electronic devices to perform optical-to-electrical conversion as part of the monitoring process. Therefore, when data rates exceed 40 Gb/s per channel these electronic OPM schemes become impractical due to the limitation imposed by the electronic bandwidth.

All-optical performance monitoring based on nonlinear optics, which does not require high-speed electronic devices, is an alternative and attractive solution for high bitrates of 40 Gb/s and beyond which provides ultrahigh resolution due to the femtosecond response time of Kerr nonlinear effect [9]. Various all-optical architectures have been demonstrated to measure impairments of a signal under test (SUT), namely radio-frequency (RF) spectrum monitoring based on cross-phase modulation (XPM) [10,11], cascaded four-wave mixing [12], semiconductor optical amplifier based optical regeneration [13], a nonlinear optical loop mirror [14] and data stream intensity autocorrelation [15]. However these techniques have limited dynamic range or do not perform simultaneous multi-impairment monitoring, which is critical in optical networks.

We recently demonstrated an OPM technique to simultaneously monitor group velocity dispersion (GVD) and in-band optical signal to noise ratio (OSNR) of an optical signal [16]. Our approach was based on measurement of the RF spectrum obtained using cross-phase modulation. We then retrieved the autocorrelation (AC) waveform of the SUT which yielded the individual impairments. Although impressive results were obtained, the low nonlinear

#119870 - $15.00 USD Received 11 Nov 2009; revised 28 Jan 2010; accepted 9 Feb 2010; published 12 Feb 2010

response of silica highly nonlinear fiber (HNLF) meant its length had to be hundreds of meters to provide sufficient nonlinearity and this led to significant walk-off between the SUT and the cw probe [9] notably reducing the measurement bandwidth. Furthermore, a fiber approach is incompatible with integration and does not offer a low cost solution. Photonic integration, on the other hand, would offer a compact and low-cost approach and the potential to incorporate multiple functions on a monolithic platform.

In this paper we present a novel multiple impairment all-optical performance scheme based on a photonic-chip based RF spectrum analyzer (PC-RFSA) for ultrahigh bitrates. We employ a 7-cm highly nonlinear (γ ≈9900 /W/km), dispersion-engineered ChG waveguide chip, which offers dramatically increased bandwidth due to reduced walk-off [11]. We apply this scheme to monitor GVD, in-band OSNR and timing jitter of 640 Gb/s return-to-zero (RZ) signals with an OSNR measurement dynamic range of greater than 30 dB. Our approach allows flexible wavelength operation, high measurement sensitivity without complex interferometric alignment. It also offers the capability for multi-impairment monitoring of up to Tb/s optical signals from a single measurement.

2. Working principle and waveguide

There are two main components to this multi-impairment monitoring approach. The first is to capture the RF spectrum and autocorrelation (AC) trace of a signal under test (SUT) from a single measurement with the PC-RFSA. The second is the monitoring algorithm used to extract impairment signatures from the RF spectra/AC traces.

Figure 1(a) shows the conceptual diagram to obtain the RF spectrum and AC waveform of the SUT [10,11,16]. Firstly, the RF spectrum is captured by co-propagating the signal at frequency f_s with a weaker cw probe at frequency f_p through the nonlinear waveguide. The sidebands generated around the probe due to XPM [9] are proportional to the power spectrum of the signal intensity [10,11]. Thus the RF spectrum of a SUT can be fully captured on an optical spectrum analyzer (OSA). Based on the Weiner-Khintchine theorem, we utilize the complete RF spectrum to generate the AC waveform by a numerical inverse Fourier transform (IFT) operation [17,18].

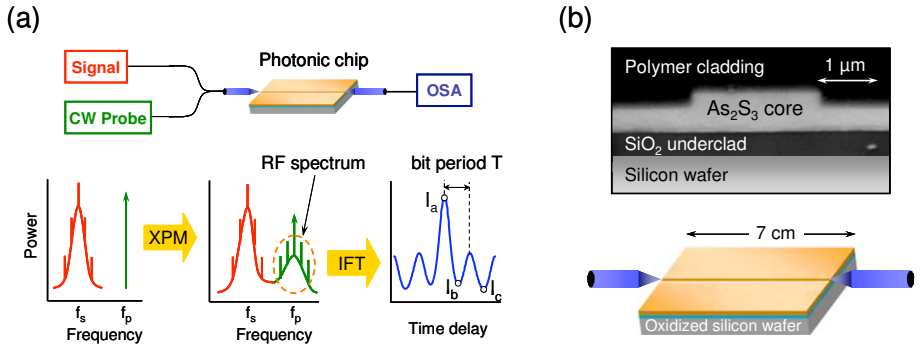

Fig. 1. (a) Schematic of simultaneous multi-impairment monitoring based on THz bandwidth PC-RFSA [11,16]. IFT relates the RF spectrum to the AC waveform. (b) (Upper) Optical micrograph of ChG planar waveguide cleaved facet and (lower) circuit schematic of the 7cm chip.

We employ two techniques to enhance the AC waveform reconstruction. Firstly, we perform a measurement calibration to eliminate the background in the retrieved AC trace of the un-distorted SUT (with no GVD and high OSNR) based on the fact that the ratio between autocorrelation and cross-correlation (XC) peaks is approximately 2 in a true PRBS sequence. We then applied this for other AC waveform reconstructions, without the need of considering the autocorrelation and XC peaks ratio again. Secondly, the temporal resolution of the experimental AC waveform, which is determined by the sampling point time step [18], is

#119870 - $15.00 USD Received 11 Nov 2009; revised 28 Jan 2010; accepted 9 Feb 2010; published 12 Feb 2010

improved by extending the bandwidth of the captured RF spectrum with a numerically generated noise floor.

The key device to our approach is a dispersion-shifted As_2S_3 planar waveguide which offers both high Kerr nonlinearity and low dispersion over the C- and L-bands. Chip fabrication involves depositing a 0.85 μm thick film of As_2S_3 on an oxidized silicon wafer. A 7 cm long straight rib (2 μm wide), whose optical micrograph of cleaved facet and circuit schematic are shown in Fig. 1(b), is formed by photolithography and dry-etching. The chip is protected by a polymer layer before depositing an anti-reflection coating on the cleaved facets to minimize Fabry-Perot reflections. The effective core area A_{eff} of the fundamental transverse magnetic (TM) mode of this waveguide is reduced to ~1 μm^2 to enhance its nonlinearity (γ ~9900 /W/km) and shift the zero dispersion wavelength closer to 1550 nm. This short and low dispersion waveguide reduces the walk-off [9], permitting high measurement bandwidth. This permits a broad bandwidth and results in low signal waveform distortion, thus high RF spectral measurement accuracy [18].

Our monitoring approach is based on the relationship between signal impairments and their RF spectra/AC traces, as shown in Fig. 2(a)–2(c). Firstly, GVD disperses the SUT, thus reducing the peak intensity, which leads to interference between adjacent pulses. This produces ripples on the RF spectrum and results in the peak intensity at zero delay dropping together with an increase of the dips at T/2 and 3T/2 delays on the AC waveform [15]. ASE noise, on the other hand, decreases XPM efficiency and increases the noise floor on the RF spectrum, thus creating a constant background intensity on the AC trace [15]. Timing jitter of a SUT produces phase noise [19] reducing the power of higher order tones on the RF spectrum. It also broadens the width of the cross-correlated pulses whilst not affecting the zero-delay autocorrelation waveform [15,20]. Note the simulation results are discussed assuming that the pulse shape is Gaussian.

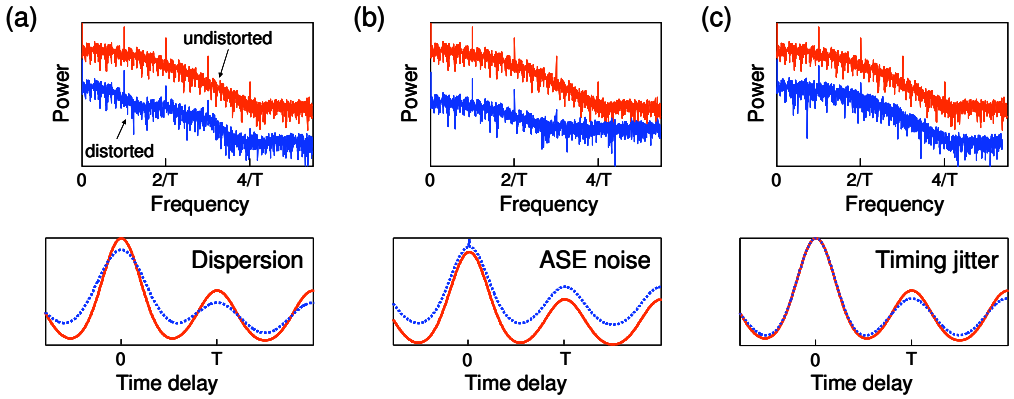

Fig. 2. Numerical (upper) RF spectra and (lower) AC waveforms of undistorted (solid) and distorted (dotted) signal due to (a) dispersion, (b) ASE noise, and (c) timing jitter. T is the bit period of the simulated SUT.

We propose an algorithm to determine the impairments in three key steps. In step one, the dispersion is obtained from the AC trace. Once GVD is determined, the OSNR is detected in step two by measuring the optical clock tone captured from the PC-RFSA to take advantage of its much higher dynamic range. In step three, the *root-mean-square* (*rms*) value of timing jitter is calculated from the reconstructed AC waveform as reported in [20,21]. Here we introduce a more robust timing jitter calculation (assuming a SUT has Gaussian shape) which is expressed in terms of full-width at 90% maximum $T_{90\%\text{-AC}}$ and $T_{90\%\text{-XC}}$ of the autocorrelation and cross-correlation peaks $J_{rms} = 1/\left[4\sqrt{-\ln(0.9)}\right] \times \sqrt{T_{90\%-XC}^2 - T_{90\%-AC}^2}$.

#119870 - $15.00 USD Received 11 Nov 2009; revised 28 Jan 2010; accepted 9 Feb 2010; published 12 Feb 2010

3. Experiment

Our experimental setup is shown in Fig. 3(a). A 40 GHz train containing ~550 fs duration pulses (λ_s = 1543 nm) was generated from a mode-locked fiber laser (MLFL) followed by nonlinear pulse compression. This was encoded with data using a Mach-Zehnder (MZ) modulator driven electrically by a 40 Gb/s pseudo-random bit sequence (PRBS) of 2^{31} - 1 pattern length. Optical time-division multiplexing (MUX) in a four-stage fiber delay line interferometer of 2^7 - 1 bit delay produced a 640 Gb/s signal (~35% duty cycle). The eye diagram and the optical spectrum of this 640 Gb/s signal is shown in Fig. 3(i) and Fig. 3(b), respectively. Impairments were simulated by adding GVD from a Finisar WaveShaper [22] and ASE noise from an erbium doped fiber amplifier (EDFA). The SUT and polarized ASE noise (after the in-line polarizer) were filtered with 8 nm bandwidth filters before co-propagating with a cw probe (that was also filtered by a 0.7 nm filter). The distorted 640 Gb/s optical signal (P_{ave} = 70 mW) and a cw probe (P_{ave} = 30 mW, λ_p = 1580 nm) were launched into a 7-cm-long dispersion-engineered As_2S_3 planar waveguide (γ ≈9900 /W/km, dispersion D ≈28 ps/nm/km at 1550 nm). Note the polarization controllers (PCs) help to couple to the fundamental TM mode of the waveguide (insertion loss ≈14.2 dB) via a pair of lensed fibers with 2.5 μm spot diameter. An example of the captured RF spectrum and the numerically reconstructed AC waveform of a 640 Gb/s optical signal is shown in Fig. 3(c), 3(d), respectively.

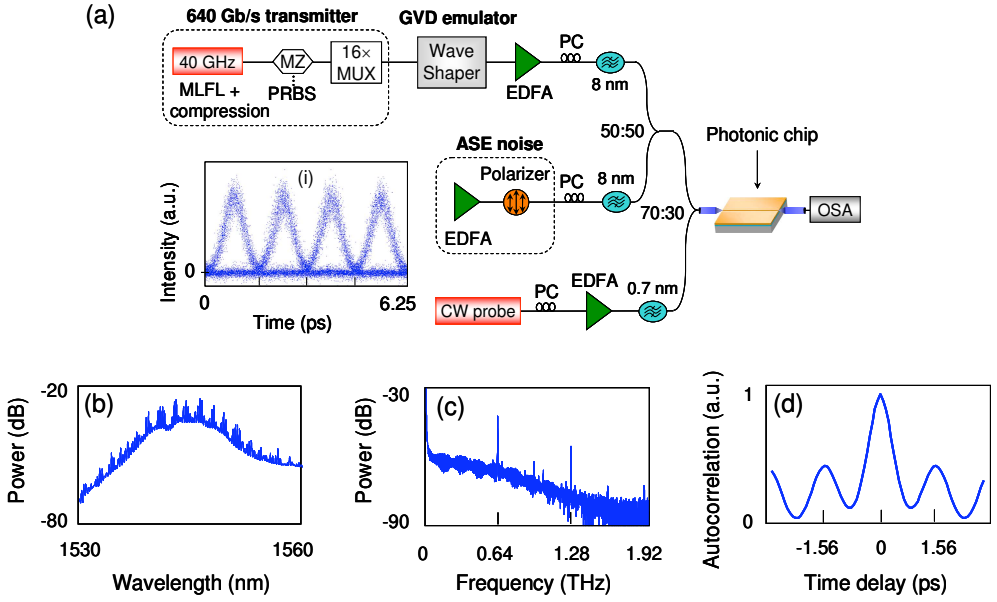

Fig. 3. (a) Experimental setup for simultaneous multi-impairment monitoring; (i) an eye diagram of a 640 Gb/s optical time division multiplexing source signal. (b) The optical spectrum, (c) the captured RF spectrum via PC-RFSA and (d) corresponding reconstructed AC waveform of a 640 Gb/s optical signal.

Figure 4 experimentally demonstrates the effect of dispersion and ASE noise impairments on the AC waveforms. Here we show contours plots of the normalized AC traces reconstructed from the captured RF spectra for various GVD and OSNR values. We define I_a, I_b and I_c as AC power at zero, 0.5T and 1.5T delays respectively, where T is the bit period of a 640 Gb/s signal. In the case of increasing GVD from 0 to 0.16 ps/nm (with OSNR ~40 dB), the AC peak intensity (I_a - I_b) reduces while the bit asymmetry (I_b – I_c) increases as shown in Fig. 4(a). These trends reverse as the GVD is increased further from 0.16 to 0.21 ps/nm due to the reconstruction of periodic signals that can be explained by the temporal Talbot effect [23]. In contrast to GVD, the AC peak intensity increases while bit asymmetry remains fairly

#119870 - $15.00 USD Received 11 Nov 2009; revised 28 Jan 2010; accepted 9 Feb 2010; published 12 Feb 2010

constant when the OSNR is reduced from 40 to 0 dB (with GVD ~0 ps/nm) [Fig. 4(b)]. Similar to Fig. 4(b), 4(c) depicts AC traces with varying OSNR, but with GVD ~0.08 ps/nm. Here we can see different features compared with the case of zero GVD. To summarize, different forms and amounts of impairments reflect differently on the corresponding AC waveforms, and this is exploited for multi-impairment OPM.

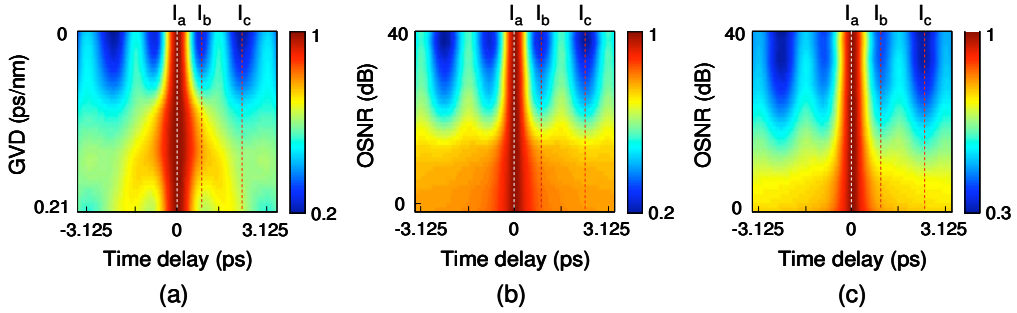

Fig. 4. (a) Experimental results showing the top view of the retrieval AC waveforms of 640 Gb/s optical signals while varying (a) GVD (OSNR ~40 dB), (b) OSNR (GVD ~0 ps/nm) and (c) OSNR (GVD = 0.08 ps/nm).

We apply this monitoring scheme to simultaneously monitor impairments on a 640 Gb/s signal caused by GVD, ASE noise and timing jitter. Firstly, GVD is distinguished based on the specific features of the AC traces described above. In Fig. 5(a), we map the AC peak intensity ($I_a - I_b$) against the AC bit asymmetry ($I_b - I_c$). Each point on this map uniquely defines both OSNR and GVD values; thus we can determine both GVD and OSNR values from this graph. However, the dynamic range of the OSNR measurement obtained from the AC traces is small (< 3 dB [15]) compared to > 30 dB output range measured from the fundamental 640 GHz clock tone of the RF spectrum, as shown in Fig. 5(b). Note that GVD = 0 ps/nm in the OSNR measurements shown in Fig. 5(b). Therefore, once GVD has been determined in step one; we enhance the OSNR monitoring performance by measuring the optical tone power (plotted in Fig. 5(c) as a function of OSNR). We also note that all GVD and OSNR used in these measurements are true values as they were calibrated and measured directly from the waveshaper and OSA respectively.

Finally, timing jitter results are plotted in Fig. 5(d), showing a low timing jitter of ~100 fs (in the case of no other impairments) for our 640 Gb/s optical signal. Furthermore, the impact of the GVD and OSNR degradation on the quality of the SUT is also demonstrated. Figure 5(d) clearly shows that with increasing GVD and ASE noise, timing jitter increases as we expect. With the appearance of other impairments such as GVD and ASE noise, the true timing jitter J_{true} is obtained from both $J_{measure}$ and $J_{distort}$ as $J_{true} = \sqrt{J_{measure}^2 - J_{distort}^2}$ [24], where $J_{measure}$ is calculated from the experimental AC waveform and $J_{distort}$ refers to a numerically calculated timing jitter of a simulated zero-jitter-source with the same GVD and OSNR as measured previously. For comparison, Fig. 5(d) also depicts timing jitter measurements using an optical sampling oscilloscope (OSO), showing a good agreement between two methods.

#119870 - $15.00 USD Received 11 Nov 2009; revised 28 Jan 2010; accepted 9 Feb 2010; published 12 Feb 2010

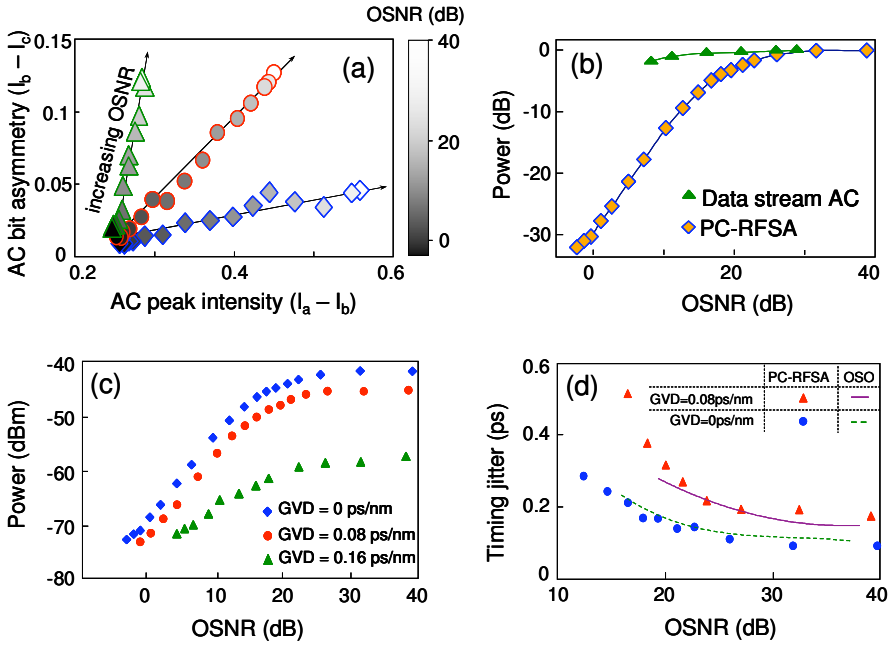

Fig. 5. (a) Step 1 – GVD measurement (GVD = 0 (diamond), 0.08 (circle) and 0.16 (triangle) ps/nm). The arrows show directions of increasing OSNR values. (b) OSNR monitoring using PC-RFSA and data stream AC [15] methods, highlighting very large dynamic range of PC-RFSA scheme. The lines are to guide the eye. (c) Step 2 – OSNR monitoring via optical tone power once GVD is determined. (d) Step 3 – timing jitter measurements once GVD and OSNR are obtained from step 1 and 2.

4. Discussion

There are significant performance advantages of this PC-RFSA based multi-impairment monitoring scheme. Firstly, analyzing the AC waveform obtained from a broadband RF spectrum measurement offers simultaneous multi-impairment measurement without ambiguities and a large OSNR measurement dynamic range of > 30 dB. Conventional AC measurements are limited by the dynamic range of the oscilloscope trace and are less robust due to complex interferometric alignment. Secondly, the PC-RFSA based on the short, highly nonlinear and dispersion-shifted planar waveguide offers broad bandwdith (> 2 THz) due to very low walk-off between the SUT and the cw probe leading to high measurement accuracy and good temporal resolution of tens of femtoseconds [18]. This allows the RF spectra/AC waveforms of 640 Gb/s signals to be captured accurately. Thirdly, the timing jitter results obtained using the PC-RFSA method represent the true timing jitter in the system, while the jitter measured using an optical sampling oscilloscope (OSO) is affected by the influence of amplitude fluctuations [25]. The limited temporal resolution of the OSO (> 600 fs) not only restricts the operating bitrates but also produces jitter measurement errors for data rates of ≥ 640 Gb/s.

We note that the GVD monitoring window for a 640 Gb/s RZ signal is currently limited to about ± 0.16 ps/nm because of the reconstruction of periodic signals. However, this monitoring window can be expanded by further analyzing the RF spectra/AC waveforms. The current monitoring speed is ultimately determined by the sweeping time of the OSA. Finally, the required input power can be significantly reduced by decreasing insertion loss and enhancing the nonlinear coefficient of the ChG planar waveguide. Placing the monitor after an in-line EDFA within the network will further reduce the power requirement.

#119870 - $15.00 USD Received 11 Nov 2009; revised 28 Jan 2010; accepted 9 Feb 2010; published 12 Feb 2010

5. Conclusion

We have demonstrated simultaneous multi-impairment monitoring of 640 Gb/s optical signals based on PC-RFSA. The novel feature of this approach is the combination of the captured RF spectra and AC traces, which provides excellent output dynamic range and resolves the measurement ambiguities arising from simply measuring the optical tone power from the RF spectrum. By exploiting the high nonlinearity and low dispersion of a ChG photonic chip, large measurement bandwidth, high accuracy/low signal distortion and operating wavelength flexibility have been achieved. These features allow the capture of RF spectra/AC waveforms of broadband optical signals within the whole C- and L-band correctly. Finally, we have demonstrated the effectiveness of this scheme as a useful diagnostic tool for multi-impairment monitoring of up to terabit data rates.

Acknowledgement

This work was supported by an Australian Research Council (ARC) under the ARC Centres of Excellences and Linkage Programs.

#119870 - $15.00 USD Received 11 Nov 2009; revised 28 Jan 2010; accepted 9 Feb 2010; published 12 Feb 2010